INT. J. REMOTE SENSING, 1998, VOL. 19, NO. 17, 3383–3397

Detection of shoreline changes for tideland areas using multi-temporal satellite images

L. C. CHEN and J. Y. RAU

Center for Space and Remote Sensing Research, National Central University, Taiwan, Republic of China

(*Received 3 January 1997; in final form 25 June 1997*)

Abstract. An original scheme to detect shoreline changes using multi-temporal satellite images and tidal measurements is presented here. First, the basic idea behind this investigation is to reconstruct a reference digital terrain model (DTM) for tideland areas from a set of SPOT satellite images sampled over a short period. Each image corresponds to a tidal measurement. Then, the shoreline, as interpreted from a historical satellite image, is compared with one traced from the reference DTM, according to the associated tidal elevations. Experimental results indicate that the area error of the test sand barriers ranges between 7.6% and 12.5%.

1. Introduction

Detection and measurement of terrain and landcover changes for coastal zones is an important task in environmental monitoring. Shoreline variations have a direct impact on economic development and land management. Thus, terrain changes in tideland areas have attracted world-wide interest (Welch *et al.* 1992, Stokkom *et al.* 1993). Approaches for detecting shoreline changes may be roughly divided into three categories: ground surveying, modern altimetric technology, and image measuration. For ground surveying, although high accuracy is possible, it is labour intensive and time consuming. For the newer altimetric technology which uses radar altimeters or laser altimeters has a high potential. However, those detectors are currently less available. For image measuration, airborne imagery provides sufficient pictorial information. Nevertheless, the photogrammetric procedure including data acquisition and data reduction is costly and also time consuming to a certain degree. Satellite imagery, on the other hand, has a larger ground coverage and a revisit capability. In addition, satellite images could be multi-spectral from optical sensors or with multi-frequency/multi-polarization for synthetic aperture radar (SAR) images. An important trend for earth resource satellites is that the spatial resolution is getting higher and higher. Accordingly, satellite imagery provides a good alternative for detecting shoreline changes due to its general availability, large ground coverage, sufficient information contents, and the trend of higher spatial resolution.

Carter (1978) investigated the applicability of satellite images for data collection on wetlands. The spatial resolution of the satellite images, (i.e. Landsat-MSS), was limited to 80 m, at the time. Frihy *et al.* (1994) identified the pattern of shoreline changes in the Nile Delta. However, the dynamic tidal variation was not treated rigorously. Accordingly, three-dimensional terrain analysis for shore areas was not considered. The spatial and temporal resolutions of satellite images have significantly improved in recent years. Thus, the applicability of the images to coastal zone

monitoring becomes more promising. One of the fundamental problems in detecting shoreline changes is that we can compare multi-temporal image shorelines only when they have been normalized to a common tidal elevation.

Chen *et al.* (1995) reported a zero-order approach, detecting shoreline changes on the west coast of Taiwan. In this approach, two SPOT images, sampled at two instances, were compared directly when the two images have similar tidal elevations. This approach is easy to implement. However, from a real application point of view, two images acquired with similar tidal elevations cannot always be expected. For three-dimensional modelling we propose a scheme that would overcome the limitations of two-dimensional processing encountered by current approaches. The basic idea is to first reconstruct a reference DTM for the tideland area of interest from a set of reference satellite images and tidal measurements. The reference DTM represents the terrain of the tideland area of the time when reference satellite images were acquired. Then, the shorelines were extracted from a historical target satellite image and compared to the ones traced from the reference DTM, according to the associated tidal elevations. In reconstructing the reference DTM, the following assumptions were made. First, the terrain variations in the tideland area are insignificant over the short period when the reference satellite images are acquired, and the measurements of tidal elevations for the tideland area in each image are available.

2. The proposed scheme

The proposed scheme has two major components. The first is the derivation of a reference DTM from a set of SPOT images, incorporating the associated tidal heights. The second component involves tracing the shoreline, according to the tidal elevation of a historical target image, from the reference DTM. Thus, a change in a shoreline may be detected by comparing the traced shoreline with its counterpart in a historical target image. Considering the local tidal height variation, at an instant provided by the SHM(Simplified Harmonic Method) (Hydrographer of the Navy 1992), the tracing procedure needs to be scrutinized. A flowchart of the proposed scheme is shown in figure 1. Although SPOT images are used in this investigation, the proposed scheme is not limited to optical images. The proposed idea of three-dimensional modelling for tideland areas may also be applied when SAR images are utilized.

2.1. *Generation of a reference DTM*

The procedure for the derivation of a reference DTM includes:

1. Collecting a reference image set.
2. Performing geometrical registration among the reference images.
3. Extracting shorelines from each of the reference images.
4. Assigning elevations to each point on the extracted shorelines.
5. Generating a reference DTM grid.

Each of these steps will be discussed in turn.

2.1.1. *Collection of a reference image set*

In the selection of suitable images for data processing, the following factors were considered:

1. High spatial resolution, thus, SPOT images are selected.
2. Good image quality with little haze.

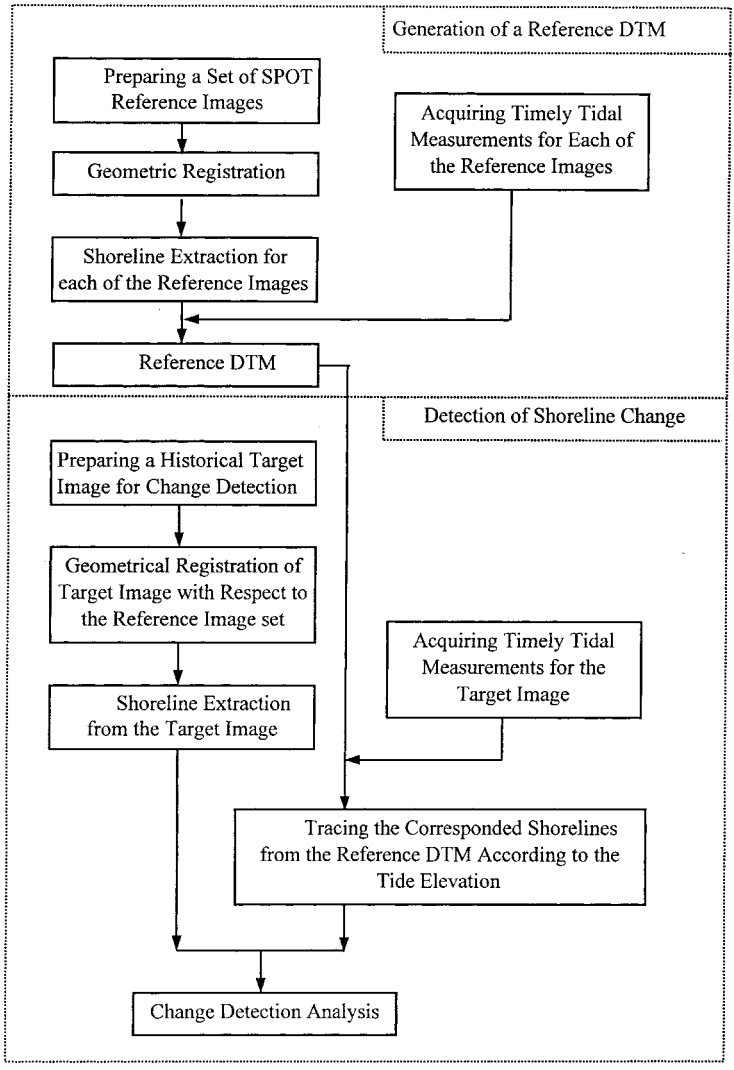

Figure 1. Flow chart of the proposed scheme.

3. Images should be sampled over a short period of time to assure that the terrain of the tideland does not change significantly.
4. Images should be associated with different tidal elevations in which the highest and lowest tides are included.

2.1.2. *Image registration*

Since the overlaying of multi-temporal images is an important step in the succeeding processes, image registration is a must. An automated procedure for image to image registration has been proposed by Chen and Lee (1992) which will be applied in this investigation. The major steps include:

1. Selecting an image as a reference.
2. The progressive generation of registration control points using feature point extraction and image matching techniques.

3. Determining transformation coefficients according to the registration control points.
4. Coordinate transformation and gray value resampling to create a new image.

If geocoded images are available for use, the first three steps are applied preferably as a geometrical check for quality control.

2.1.3. *Extraction of shorelines*

Although automated image interpretation is favoured, we select manual operation to assure reliability and accuracy. A moderate number (e.g. 100) of points are digitized on an image processing system to depict the shorelines. Multi-spectral SPOT images were used in this investigation. The reason why we selected multi-spectral images rather than panchromatic ones was due to their higher interpretability of multi-spectral, i.e. colour, images in digitizing shorelines.

2.1.4. *Elevation labelling*

The assignment of an elevation to each digitized point on the shorelines was performed according to the tidal measurements. The tidal elevation data were provided by real observations through SHM modelling (Hydrographer of the Navy 1992). Considering the local variation in tidal elevation, the data are spaced in a 1 km by 1 km grid. The elevation for each digitized point was estimated according to its four nearest grid points. In this study the height estimation included bi-linear interpolation.

2.1.5. *Generation of a reference DTM*

The reference DTM was derived in such a way that each grid elevation was calculated according to neighbouring reference points provided in the last section. The discrete points were first used to construct TINs (Triangulated Irregular Networks). Then an interpolation for each grid elevation was performed in accordance with the associated triangle (Lee and Chen 1990).

2.2. *Change detection for shorelines*

Once the reference DTM for the time, $T1$, was reconstructed, a historical satellite image, sampled at time $T2$, could be targeted to analyse the shoreline changes between $T1$ and $T2$. The processing steps were:

1. Registering a $T2$ image on the $T1$ coordinate system.
2. Digitizing the shorelines on the $T2$ image.
3. Tracing 'corresponding shorelines' from the reference DTM according to the tidal elevation at $T2$.
4. Comparing the lines derived from steps 2 and 3 to detect changes.

Steps 1 and 2 may be accomplished as stated in the previous section, while step 4 is straightforward. Thus, we will concentrate on step 3.

In essence this step actually traces the contour lines from the reference DTM. As stated in the previous sections, the grid elevation data provided by the SHM considers local variations at any instant. This makes the tracing of corresponding shorelines as contour lines with equal elevation impractical. We developed a technique, illustrated in figure 2, to overcome this difficulty.

A corresponding shoreline was traced by finding the intersecting line between the reference DTM and the tidal surface. To accomplish this, we first selected a

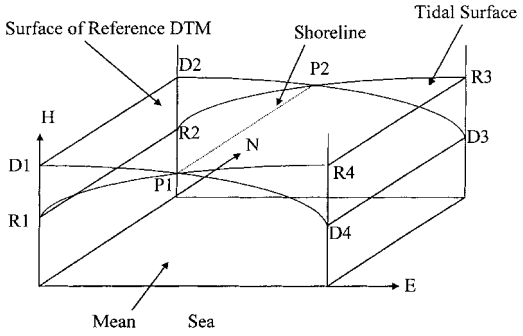

Figure 2. An illustration of datum transformation in shoreline tracing.

second-order polynomial

$$H = a_0 + a_1 E + a_2 N + a_3 EN + a_4 E^2 + a_5 N^2, \tag{1}$$

where H= elevation, E, N= planimetric coordinates, and $a_0 \sim a_5$= coefficients, to fit a surface (R_1, R_2, R_3, R_4) for the tidal elevation data, with a grid size of 1 km by 1 km. When the coefficients were determined, we then reduced the elevation for each pixel in the reference DTM (D_1, D_2, D_3, D_4) with the value derived from equation (1) according to the planimetric coordinates. The following step of shoreline tracing was then simplified after elevation reduction to the location of the zero crossings in the reference DTM.

The next step was to compare the real shorelines on the $T2$ image to the corresponding one extracted from the reference DTM according to the tidal elevation at time $T2$. In addition to the visual inspection, the comparison may be quantified in two ways. The shoreline change may be demonstrated by the sum of the norms for each point along the real shoreline with respect to the corresponding shoreline. The difficulty in this evaluation is that two lines are sometimes shaped so differently that the evaluation cannot be fully automated due to the 'norm' not being well defined. Thus, the quantitative evaluation used in this study is to observe the area change.

3. Quantitative evaluation

To indicate the proposed scheme's performance, two quantitative checks of the results were examined. The first is called the self-consistency check and the second, the absolute check. Similar to that discussed in the last section, the area variations will be considered as the error index. Referring to figure 3, the areas of regions, A, B, and C bounded by the real and the traced shorelines, were accumulated. The total area was used as the error index.

3.1. *Self-consistency check*

This check reflects error propagation in the generation of the reference DTM and in shoreline tracing, for tideland areas. An image selected from the reference image set was tested, which means that when a DTM is reconstructed, one image out of the reference image set is used to compare the shoreline differences between the one digitized from the test image and the one traced from the reference DTM. Because the test image is also one of the reference images, used for terrain reconstruction, the term 'self-consistency check' is utilized.

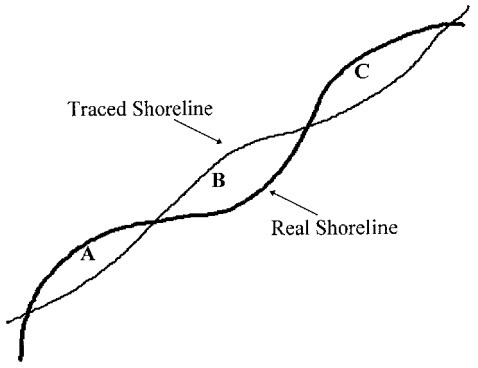

Figure 3. An illustration of error representation.

3.2. *Absolute check*

This absolute check indicates the total error accumulation including errors in image registration, shoreline digitization, tidal elevation, DTM generation, and shoreline tracing. The checking procedure is similar to that in the consistency check. The only difference is that we select an independent satellite image, sampled during the period of the reference image set, rather than directly using the reference data, as a checking target.

4. Experimental results

Tests on tideland areas covering two sand barriers, i.e. San-Tiau-Luen and Wai-San-Ting, on the western coast of Taiwan are included, to illustrate the performance of the scheme. Figure 4 depicts the location of the test sites at San-Tiau-Luen and Wai-San-Ting. The locations of four tidal stations are also illustrated. It is noticed that the two test barriers locate within the four tidal stations. Thus, the sea surface modelling using SHM is in essence an interpolating computation. That means an extrapolation has been avoided to assure the model fidelity. Five SPOT multispectral images were acquired to be used as reference images. Figure 5 shows the five images, sampled in 1994, on which the extracted shorelines are superimposed. A historical target image was acquired in 1986 for change detection (figure 6). The sampling times and the associated tidal elevations for each image are indicated in table 1. The tidal elevation provided by the SHM is a set of grid data, with a 1 km × 1 km resolution. Thus, each elevation in table 1 is actually nominal.

For both test sites, the five images in figure 5 were used as the reference image data set for DTM reconstruction. Image *D* was selected as a test image in a consistency check. For an absolute check, on the other hand, image *D* was only treated as a test image without being used in the DTM reconstruction.

All of the test images were geocoded and resampled to a 12.5 m by 12.5 m pixel spacing. To assure further the geometrical quality of the images, a registration check was automatically performed by matching the main feature points. The rmse is smaller than 0.75 pixels, which corresponds to a ground coverage of less than 10 m.

4.1. *San-Tiau-Luen*

After superimposing the shorelines extracted from the five reference images, the reconstructed DTM is shown in figure 7. Figure 8 illustrates the difference between

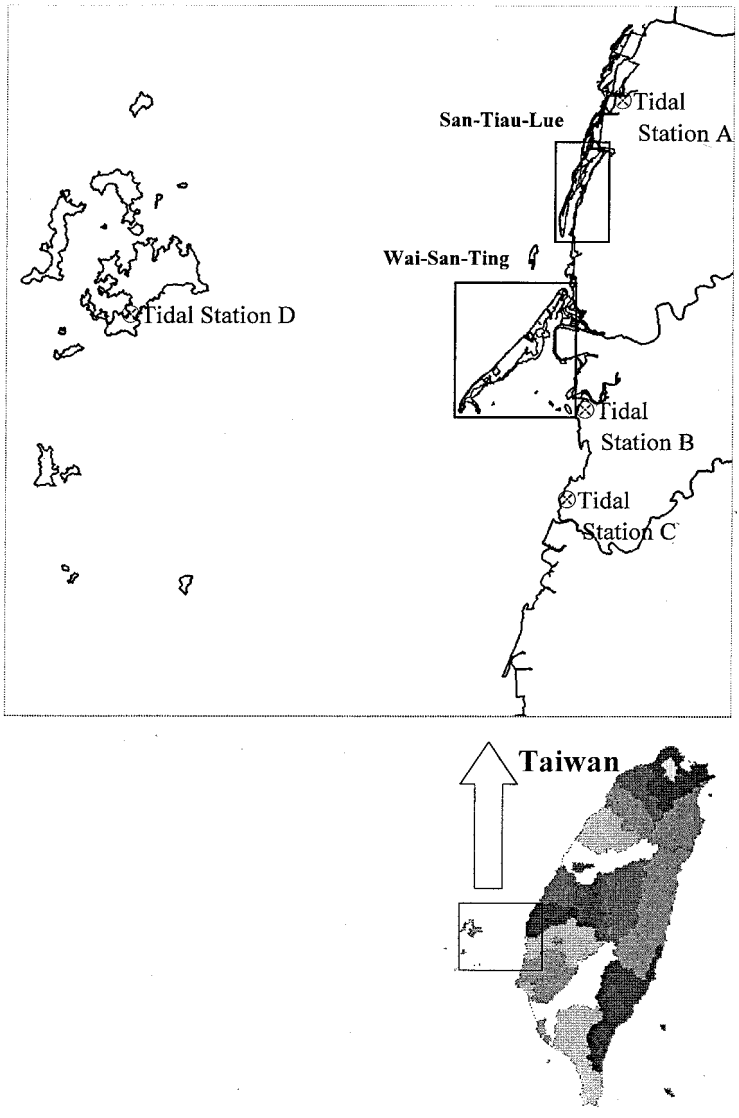

Figure 4. Test sites and tidal stations.

the traced shoreline and the real one. The area error in the consistency check is 1.4078×10^6 m^2, which corresponds to an 11.74% error with respect to the total area, of 1.1987×10^7 m^2. For the absolute check, figure 9 depicts differences in the traced and real shorelines, for which, the traced shoreline was derived from the reference DTM, when images *A*, *B*, *C*, and *E* were used. Image *D* of course, is for comparison. The area error was 1.5036×10^6 m^2, which corresponds to 12.49% of the total area.

Figure 10 delineates any shoreline change by superimposing the shoreline extracted from the historical image, i.e. in figure 6, and the shoreline traced from the reference DTM, according to the tidal elevation associated with the historical image.

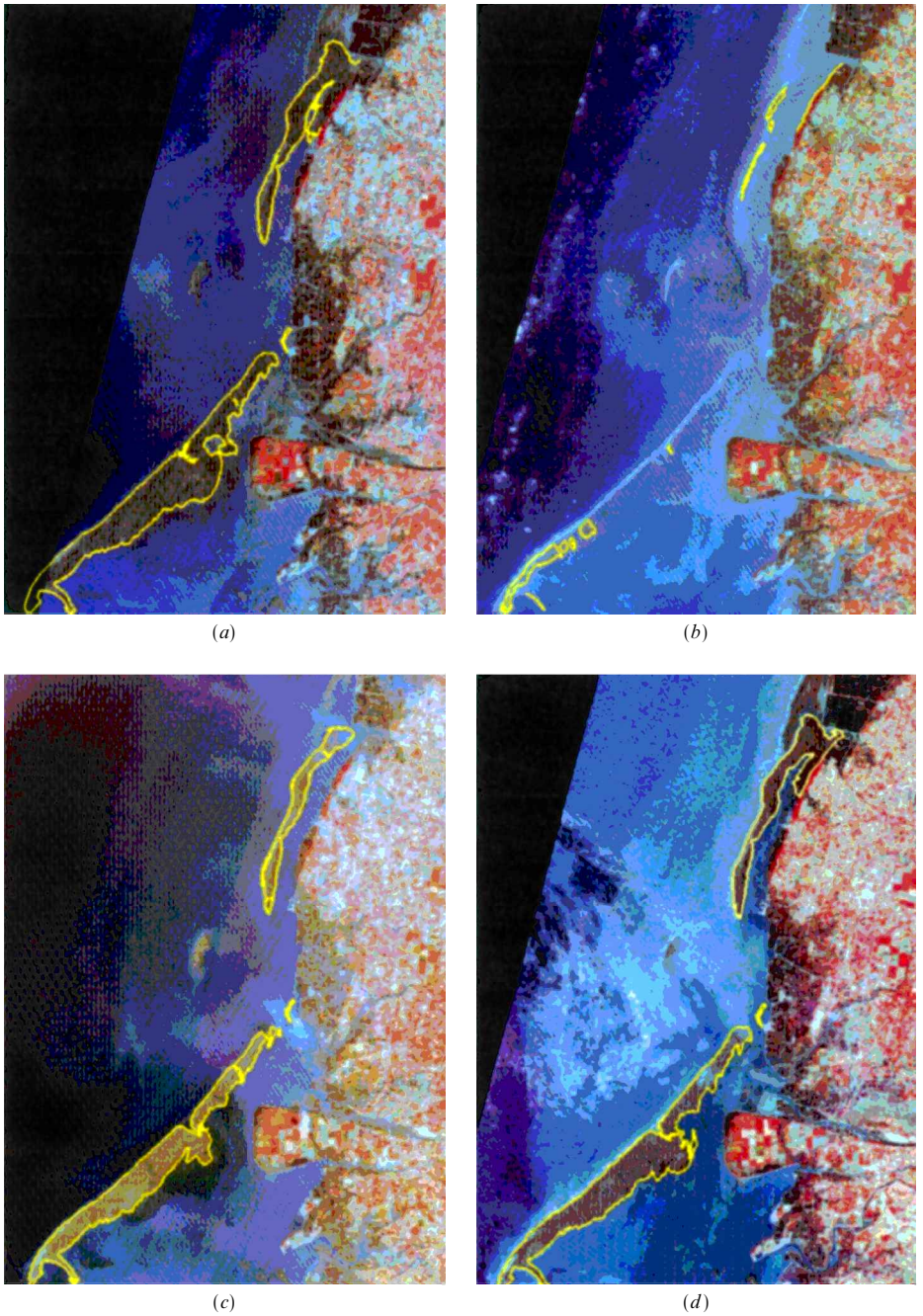

(a) (b)

(c) (d)

Figure 5. Reference images.

The total area changed from 1.7134×10^7 m^2 in 1986 to 1.0994×10^7 m^2 in 1994. This means that during the $7\frac{1}{2}$ year interval, San-Tiau-Luen lost an area of 6.14×10^6 m^2, which is equivalent to 35.84%. It should be noticed that the sand barrier changed enormously not only in the size but also in the topography as a whole.

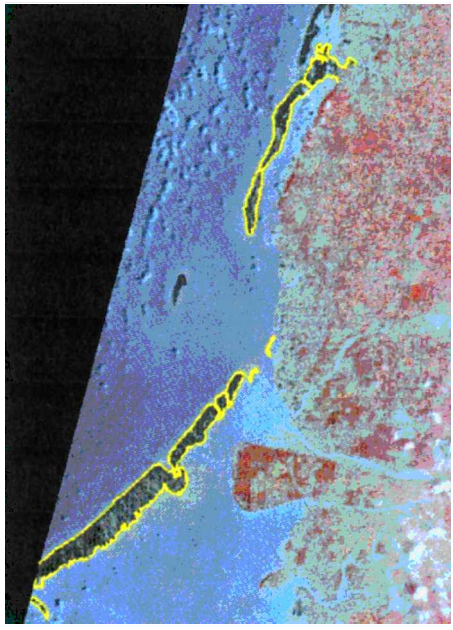

(*e*)

Figure 5. (*Cont.*)

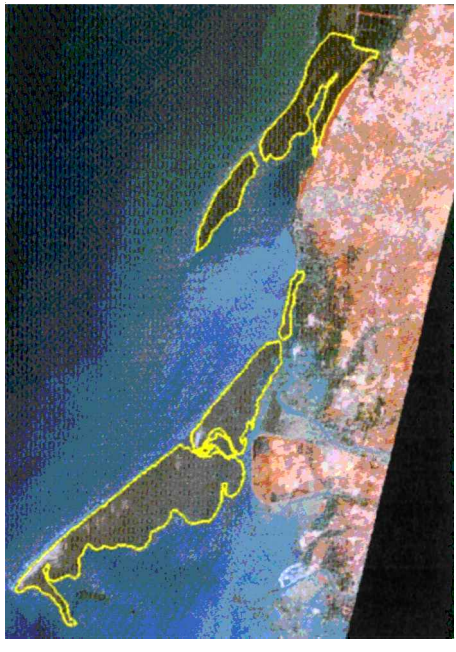

Figure 6. Historical image.

4.2. *Wai-San-T ing*

The reference DTM, reconstructed from five reference images, is shown in figure 11. Figure 12 illustrates the difference between the traced shoreline and the

Table 1. Sampling times and their associated tidal elevations.

Sampling time			Tide elevation (M)			
ID	Y-M-D	H-M-S	Station *A*	Station *B*	Station *C*	Station *D*
A	3 January 1994	10-55-53	− 0.78	− 0.26	− 0.10	− 0.79
B	11 January 1994	11-00-11	1.52	0.92	0.92	1.14
C	6 February 1994	11-00-14	0.31	0.19	0.29	0.01
D	4 March 1994	11-00-18	− 0.70	− 0.02	0.09	− 0.45
E	17 April 1994	10-56-00	− 0.24	0.39	0.41	− 0.15

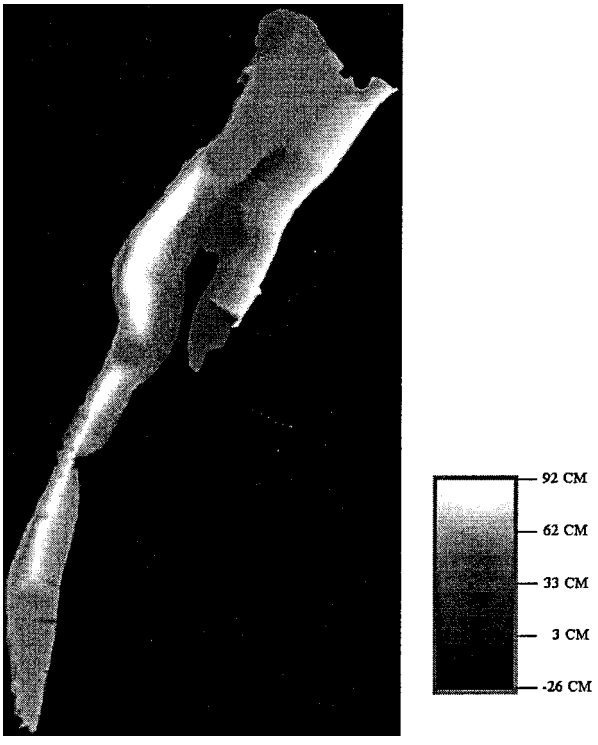

Figure 7. Reconstructed DTM for San-Tiau-Luen.

real one. The error in terms of the area, in the consistency check, is 1.409×10^6 m^2, which corresponds to a 5.52% error with respect to the total area of 2.5516×10^7 m^2. In the absolute check, figure 13 depicts differences in the traced and real shorelines. The traced shoreline was derived from the reference DTM, when images *A*, *B*, *C*, and *E* were used. The shoreline in image *D* is for comparison. The area error was 1.95×10^6 m^2, which corresponds to 7.58% of the total area.

Figure 14 delineates the shoreline change by superimposing the shoreline, extracted from the historical image, i.e. in figure 6, and the shoreline traced from the reference DTM, according to the tidal elevation associated with the historical image. It was found that during the $7\frac{1}{2}$ year interval, Wai-San-Ting lost an area of 1.745×10^7 m^2, which corresponds to 38.64% of the total area.

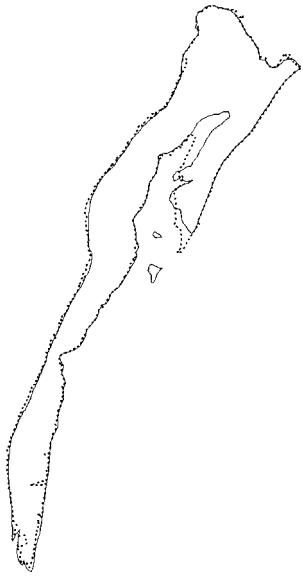

Figure 8. Verification of consistency check for San-Tiau-Luen.

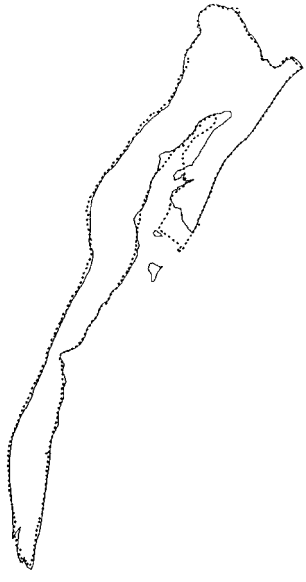

Figure 9. Verification of absolute check for San-Tiau-Luen.

4.3. *Summary of the experimental results*

1. The registration error among the test images was 0.75 pixels which corresponds to a ground coverage of less than 10 m.
2. Table 2 summarizes the results of the self-consistency check.
3. Table 3 provides the statistics for the absolute check.
4. The area changes in the test sites are compiled in table 4.

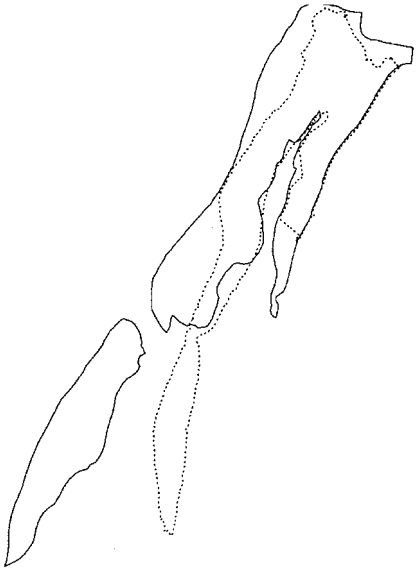

Figure 10. An illustration of shoreline change at San-Tiau-Luen.

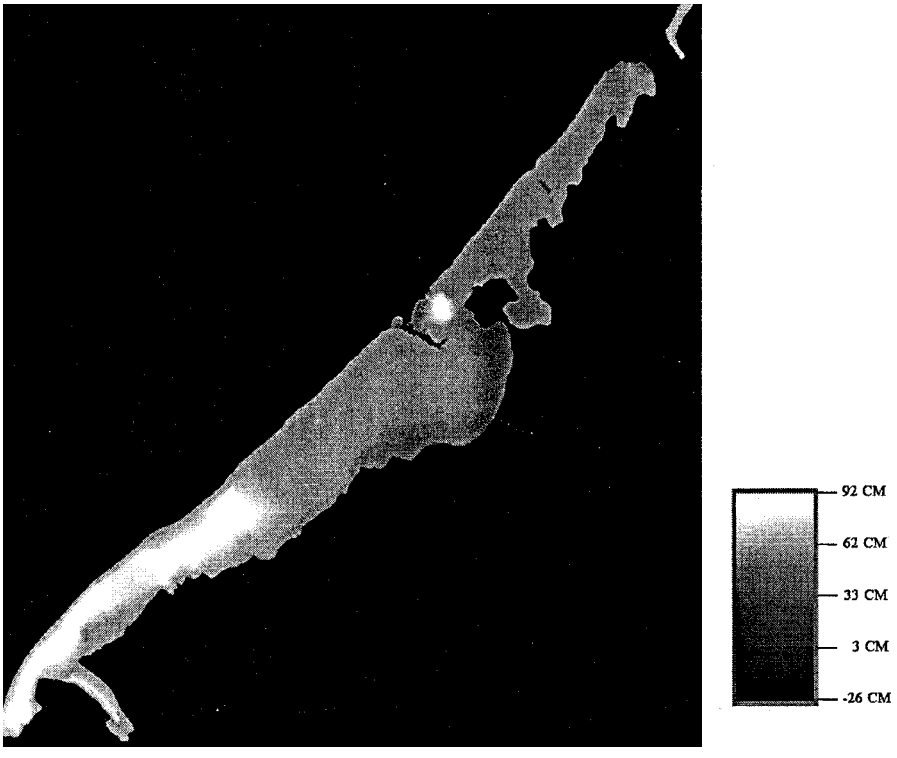

Figure 11. Reconstructed DTM for Wai-San-Ting.

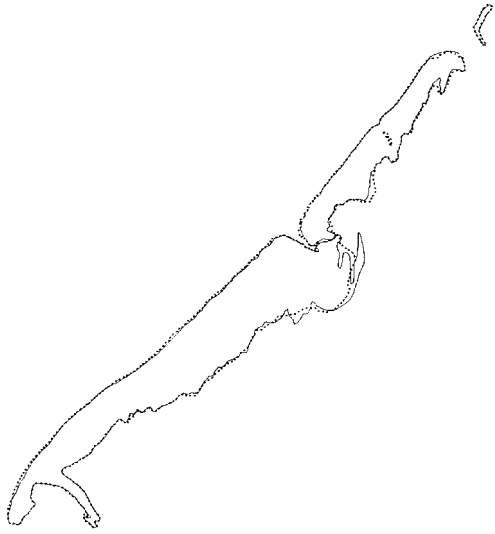

Figure 12. Verification of consistency check for Wai-San-Ting.

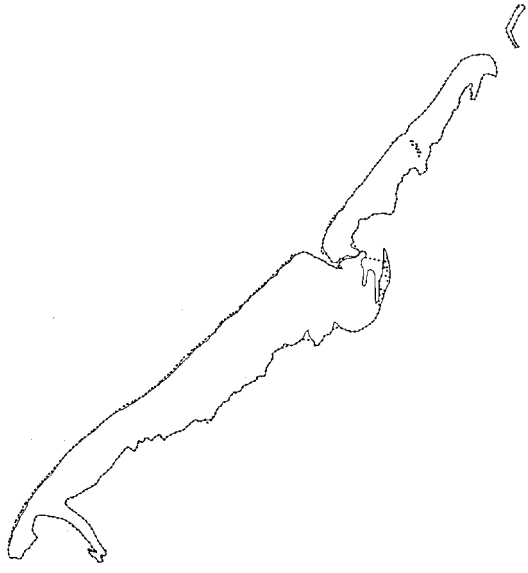

Figure 13. Verification of absolute check for Wai-San-Ting.

5. Concluding remarks

The coupling phenomenon of two dynamic factors i.e. tidal variations and terrain changes, complicates terrain analysis for tideland areas. A scheme has been proposed to cope effectively with this complexity. Quantitative verification is also provided by this paper. The features of the proposed scheme are threefold: (1) the dynamic tidal variations for shoreline change detection are considered, (2) the interrelated characteristics between shorelines extracted from a satellite image and the tidal elevations are fully utilized, and (3) three-dimensional analysis becomes possible, which means

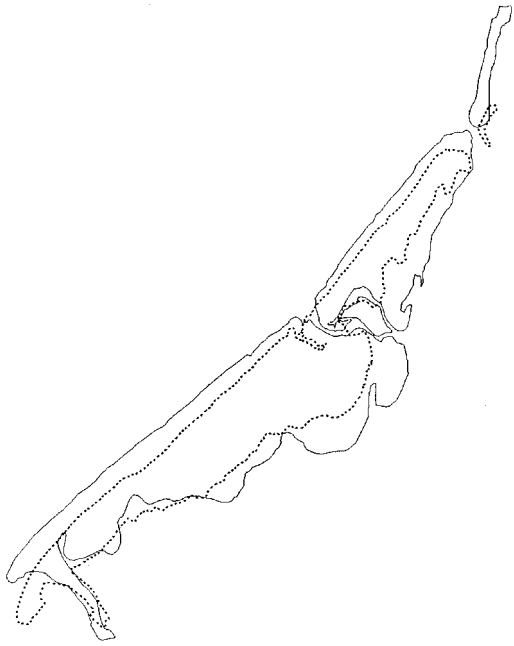

Figure 14. An illustration of shoreline change at Wai-San-Ting.

Table 2. Consistency check.

Test site	Total area (m^2)	Error (m^2)	Error percentage (%)
San-Tiau-Luen	1.1987×10^7	1.4078×10^6	11.74
Wai-San-Ting	2.5516×10^7	1.409×10^6	5.52

Table 3. Absolute check.

Test site	Total area (m^2)	Error (m^2)	Error percentage (%)
San-Tian-Luen	1.2035×10^7	1.5036×10^6	12.49
Wai-San-Ting	2.5712×10^7	1.95×10^6	7.58

Table 4. Area change.

Test site	Area in 1986 (A', m^2)	Area in 1994 (A, m^2)	Area change ($\Delta A'$, m^2)	Change rate ($\Delta A'/A'$) *100%
San-Tian-Luen	1.7134×10^7	1.0994×10^7	6.14×10^6	35.84
Wai-San-Ting	4.5156×10^7	2.7708×10^7	1.7448×10^7	38.64

that the volume change may be assessed, provided that another suitable image set which satisfies the considerations of § 2.1.1 is available. Although SPOT images were tested in this investigation, the proposed scheme is not limited to optical images.

The proposed idea of three-dimensional modelling for tideland areas may also be applied when SAR images are utilized.

The applicability of the proposed scheme relies on the temporal resolution of satellite images for constructing a reference DTM. This implies that better accuracy may be expected, provided that reference images with a higher temporal resolution are available. As more and more resource satellites are scheduled for launch in the next decade, the applicability of the proposed scheme becomes more promising.

Acknowledgements

This investigation was partially supported by the Sinotech Foundation. The authors are grateful for this support. Thanks should go to Dr C.-S. Kung, Mr B.-R. Yang, and Mr C.-G. Shieh of Sinotech Engineers Consultants Inc. for providing valuable tidal data and detail explanations.

References

CARTER, V., 1978, Coastal wetlands: role of remote sensing. *Proceedings of Symposium on Technical, Environmental, Socioeconomic and Regulatory Aspects of Coastal Zone Management, held in San Francisco, California* (New York: ASCE) pp. 1261–1284.

CHEN, L. C., and LEE, L. H., 1992, Progressive generation of control frameworks for image registration. *Photogrammetric Engineering and Remote Sensing*, **58**, 1321–1328.

CHEN, A. J., CHEN, C. F., and CHEN, K. S., 1995, Investigation of shoreline change and migration along Wai-San-Ding-Zou. *Proceedings of the 1995 International Geoscience and Remote Sensing Symposium, held in Firenze, Italy* **3** (Piscataway: IEEE), pp. 2097–2099.

FRIHY, O. E., NASR, S. M., EL HATTAB, M. M., and EL RAEY, M., 1994, Remote sensing of beach erosion along the Rosetta Promontory Northwestern Nile Delta, Egypt. *International Journal of Remote Sensing*, **5**, 1649–1660.

HYDROGRAPHER OF THE NAVY, 1992, *Admiralty Tide Tables and Tidal Stream Tables*: (The Hydrographer of the Navy).

LEE, L. H., and CHEN, L. C., 1990, Surface modeling and automated terrain feature extraction. *Proceedings of International Society for Photogrammetry and Remote Sensing Commission III Symposium, held in Tokyo, Japan*, **28**, 77–85.

STOKKOM, H. T. C., STOKMAN, G. M., and HOVENIER, J. W., 1993, Quantitative use of passive optical remote sensing over coastal and inland water bodies. *International Journal of Remote Sensing*, **14**, 541–563.

WELCH, R., REMILLARD, M., and ALBERTS, J., 1992, Integration of GPS, Remote Sensing, and GIS Techniques for Coastal Resource Management. *Photogrammetric Engineering and Remote Sensing*, **58**, 1571–1578.